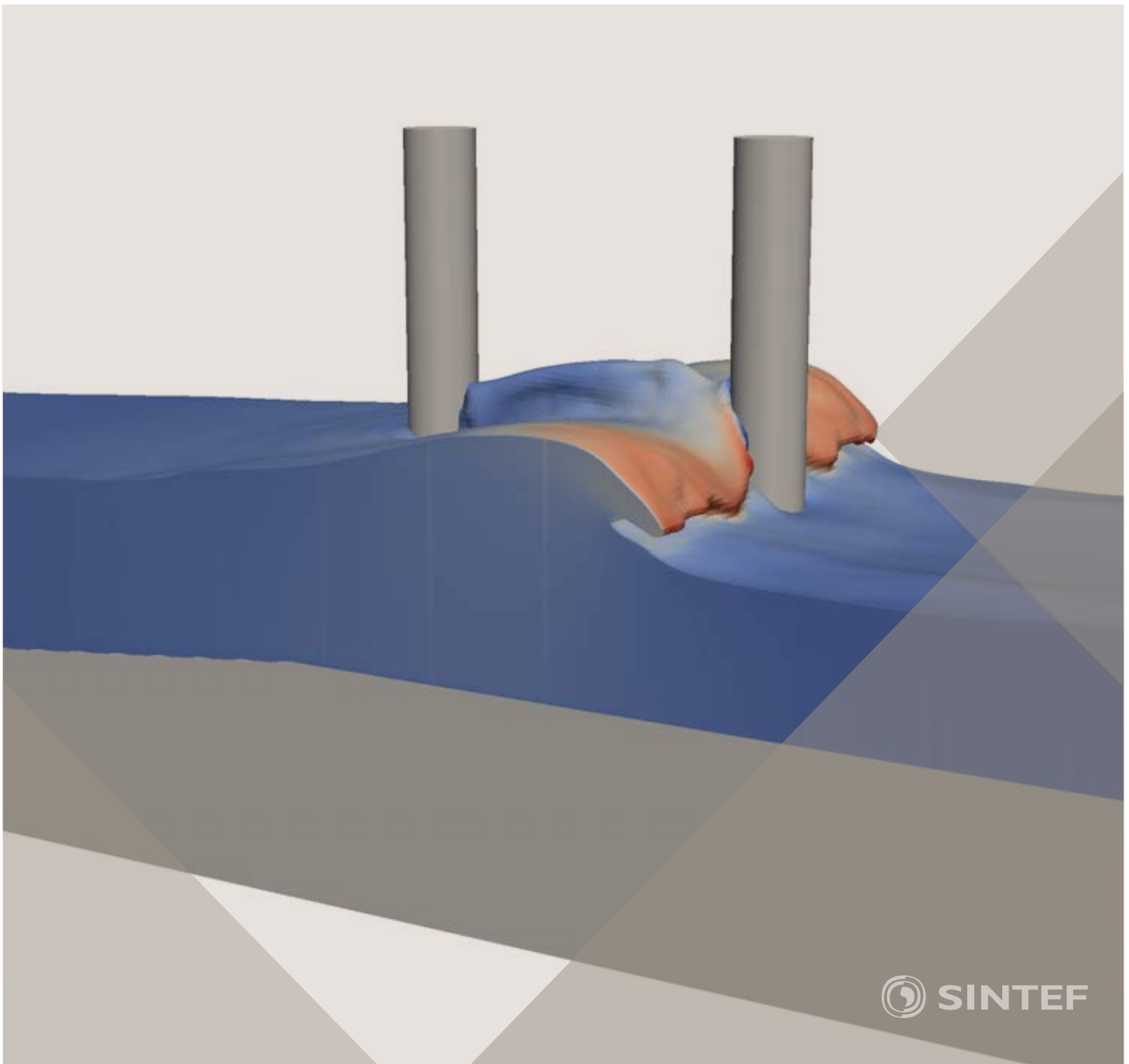


Proceedings of the 12th International Conference on
Computational Fluid Dynamics in the Oil & Gas,
Metallurgical and Process Industries

Progress in Applied CFD – CFD2017



SINTEF Proceedings

Editors:

Jan Erik Olsen and Stein Tore Johansen

Progress in Applied CFD – CFD2017

Proceedings of the 12th International Conference on Computational Fluid Dynamics
in the Oil & Gas, Metallurgical and Process Industries

SINTEF Academic Press

SINTEF Proceedings no 2

Editors: Jan Erik Olsen and Stein Tore Johansen

Progress in Applied CFD – CFD2017

Selected papers from 10th International Conference on Computational Fluid Dynamics in the Oil & Gas, Metallurgical and Process Industries

Key words:

CFD, Flow, Modelling

Cover, illustration: Arun Kamath

ISSN 2387-4295 (online)

ISBN 978-82-536-1544-8 (pdf)

© Copyright SINTEF Academic Press 2017

The material in this publication is covered by the provisions of the Norwegian Copyright Act. Without any special agreement with SINTEF Academic Press, any copying and making available of the material is only allowed to the extent that this is permitted by law or allowed through an agreement with Kopinor, the Reproduction Rights Organisation for Norway. Any use contrary to legislation or an agreement may lead to a liability for damages and confiscation, and may be punished by fines or imprisonment

SINTEF Academic Press

Address: Forskningsveien 3 B
 PO Box 124 Blindern
 N-0314 OSLO

Tel: +47 73 59 30 00

Fax: +47 22 96 55 08

www.sintef.no/byggforsk

www.sintefbok.no

SINTEF Proceedings

SINTEF Proceedings is a serial publication for peer-reviewed conference proceedings on a variety of scientific topics.

The processes of peer-reviewing of papers published in SINTEF Proceedings are administered by the conference organizers and proceedings editors. Detailed procedures will vary according to custom and practice in each scientific community.

PREFACE

This book contains all manuscripts approved by the reviewers and the organizing committee of the 12th International Conference on Computational Fluid Dynamics in the Oil & Gas, Metallurgical and Process Industries. The conference was hosted by SINTEF in Trondheim in May/June 2017 and is also known as CFD2017 for short. The conference series was initiated by CSIRO and Phil Schwarz in 1997. So far the conference has been alternating between CSIRO in Melbourne and SINTEF in Trondheim. The conferences focuses on the application of CFD in the oil and gas industries, metal production, mineral processing, power generation, chemicals and other process industries. In addition pragmatic modelling concepts and bio-mechanical applications have become an important part of the conference. The papers in this book demonstrate the current progress in applied CFD.

The conference papers undergo a review process involving two experts. Only papers accepted by the reviewers are included in the proceedings. 108 contributions were presented at the conference together with six keynote presentations. A majority of these contributions are presented by their manuscript in this collection (a few were granted to present without an accompanying manuscript).

The organizing committee would like to thank everyone who has helped with review of manuscripts, all those who helped to promote the conference and all authors who have submitted scientific contributions. We are also grateful for the support from the conference sponsors: ANSYS, SFI Metal Production and NanoSim.

Stein Tore Johansen & Jan Erik Olsen



Organizing committee:

Conference chairman: Prof. Stein Tore Johansen

Conference coordinator: Dr. Jan Erik Olsen

Dr. Bernhard Müller

Dr. Sigrid Karstad Dahl

Dr. Shahriar Amini

Dr. Ernst Meese

Dr. Josip Zoric

Dr. Jannike Solsvik

Dr. Peter Witt

Scientific committee:

Stein Tore Johansen, SINTEF/NTNU

Bernhard Müller, NTNU

Phil Schwarz, CSIRO

Akio Tomiyama, Kobe University

Hans Kuipers, Eindhoven University of Technology

Jinghai Li, Chinese Academy of Science

Markus Braun, Ansys

Simon Lo, CD-adapco

Patrick Segers, Universiteit Gent

Jiyuan Tu, RMIT

Jos Derksen, University of Aberdeen

Dmitry Eskin, Schlumberger-Doll Research

Pär Jönsson, KTH

Stefan Pirker, Johannes Kepler University

Josip Zoric, SINTEF

CONTENTS

PRAGMATIC MODELLING	9
On pragmatism in industrial modeling. Part III: Application to operational drilling	11
CFD modeling of dynamic emulsion stability	23
Modelling of interaction between turbines and terrain wakes using pragmatic approach	29
FLUIDIZED BED	37
Simulation of chemical looping combustion process in a double looping fluidized bed reactor with cu-based oxygen carriers.....	39
Extremely fast simulations of heat transfer in fluidized beds.....	47
Mass transfer phenomena in fluidized beds with horizontally immersed membranes	53
A Two-Fluid model study of hydrogen production via water gas shift in fluidized bed membrane reactors	63
Effect of lift force on dense gas-fluidized beds of non-spherical particles	71
Experimental and numerical investigation of a bubbling dense gas-solid fluidized bed	81
Direct numerical simulation of the effective drag in gas-liquid-solid systems	89
A Lagrangian-Eulerian hybrid model for the simulation of direct reduction of iron ore in fluidized beds.....	97
High temperature fluidization - influence of inter-particle forces on fluidization behavior	107
Verification of filtered two fluid models for reactive gas-solid flows	115
BIOMECHANICS.....	123
A computational framework involving CFD and data mining tools for analyzing disease in carotid artery	125
Investigating the numerical parameter space for a stenosed patient-specific internal carotid artery model.....	133
Velocity profiles in a 2D model of the left ventricular outflow tract, pathological case study using PIV and CFD modeling.....	139
Oscillatory flow and mass transport in a coronary artery.....	147
Patient specific numerical simulation of flow in the human upper airways for assessing the effect of nasal surgery.....	153
CFD simulations of turbulent flow in the human upper airways	163
OIL & GAS APPLICATIONS	169
Estimation of flow rates and parameters in two-phase stratified and slug flow by an ensemble Kalman filter	171
Direct numerical simulation of proppant transport in a narrow channel for hydraulic fracturing application	179
Multiphase direct numerical simulations (DNS) of oil-water flows through homogeneous porous rocks	185
CFD erosion modelling of blind tees	191
Shape factors inclusion in a one-dimensional, transient two-fluid model for stratified and slug flow simulations in pipes	201
Gas-liquid two-phase flow behavior in terrain-inclined pipelines for wet natural gas transportation	207

NUMERICS, METHODS & CODE DEVELOPMENT	213
Innovative computing for industrially-relevant multiphase flows	215
Development of GPU parallel multiphase flow solver for turbulent slurry flows in cyclone.....	223
Immersed boundary method for the compressible Navier–Stokes equations using high order summation-by-parts difference operators	233
Direct numerical simulation of coupled heat and mass transfer in fluid-solid systems	243
A simulation concept for generic simulation of multi-material flow, using staggered Cartesian grids.....	253
A cartesian cut-cell method, based on formal volume averaging of mass, momentum equations.....	265
SOFT: a framework for semantic interoperability of scientific software	273
POPULATION BALANCE	279
Combined multifluid-population balance method for polydisperse multiphase flows	281
A multifluid-PBE model for a slurry bubble column with bubble size dependent velocity, weight fractions and temperature.....	285
CFD simulation of the droplet size distribution of liquid-liquid emulsions in stirred tank reactors	295
Towards a CFD model for boiling flows: validation of QMOM predictions with TOPFLOW experiments	301
Numerical simulations of turbulent liquid-liquid dispersions with quadrature-based moment methods.....	309
Simulation of dispersion of immiscible fluids in a turbulent couette flow	317
Simulation of gas-liquid flows in separators - a Lagrangian approach.....	325
CFD modelling to predict mass transfer in pulsed sieve plate extraction columns	335
BREAKUP & COALESCENCE	343
Experimental and numerical study on single droplet breakage in turbulent flow	345
Improved collision modelling for liquid metal droplets in a copper slag cleaning process	355
Modelling of bubble dynamics in slag during its hot stage engineering.....	365
Controlled coalescence with local front reconstruction method	373
BUBBLY FLOWS	381
Modelling of fluid dynamics, mass transfer and chemical reaction in bubbly flows	383
Stochastic DSMC model for large scale dense bubbly flows.....	391
On the surfacing mechanism of bubble plumes from subsea gas release.....	399
Bubble generated turbulence in two fluid simulation of bubbly flow	405
HEAT TRANSFER	413
CFD-simulation of boiling in a heated pipe including flow pattern transitions using a multi-field concept	415
The pear-shaped fate of an ice melting front	423
Flow dynamics studies for flexible operation of continuous casters (flow flex cc).....	431
An Euler-Euler model for gas-liquid flows in a coil wound heat exchanger.....	441
NON-NEWTONIAN FLOWS.....	449
Viscoelastic flow simulations in disordered porous media	451
Tire rubber extrudate swell simulation and verification with experiments	459
Front-tracking simulations of bubbles rising in non-Newtonian fluids.....	469
A 2D sediment bed morphodynamics model for turbulent, non-Newtonian, particle-loaded flows.....	479

METALLURGICAL APPLICATIONS.....	491
Experimental modelling of metallurgical processes	493
State of the art: macroscopic modelling approaches for the description of multiphysics phenomena within the electroslag remelting process	499
LES-VOF simulation of turbulent interfacial flow in the continuous casting mold	507
CFD-DEM modelling of blast furnace tapping	515
Multiphase flow modelling of furnace tapholes	521
Numerical predictions of the shape and size of the raceway zone in a blast furnace.....	531
Modelling and measurements in the aluminium industry - Where are the obstacles?	541
Modelling of chemical reactions in metallurgical processes.....	549
Using CFD analysis to optimise top submerged lance furnace geometries	555
Numerical analysis of the temperature distribution in a martensic stainless steel strip during hardening.....	565
Validation of a rapid slag viscosity measurement by CFD.....	575
Solidification modeling with user defined function in ANSYS Fluent.....	583
Cleaning of polycyclic aromatic hydrocarbons (PAH) obtained from ferroalloys plant.....	587
Granular flow described by fictitious fluids: a suitable methodology for process simulations	593
A multiscale numerical approach of the dripping slag in the coke bed zone of a pilot scale Si-Mn furnace.....	599
INDUSTRIAL APPLICATIONS	605
Use of CFD as a design tool for a phosphoric acid plant cooling pond	607
Numerical evaluation of co-firing solid recovered fuel with petroleum coke in a cement rotary kiln: Influence of fuel moisture	613
Experimental and CFD investigation of fractal distributor on a novel plate and frame ion-exchanger	621
COMBUSTION	631
CFD modeling of a commercial-size circle-draft biomass gasifier.....	633
Numerical study of coal particle gasification up to Reynolds numbers of 1000.....	641
Modelling combustion of pulverized coal and alternative carbon materials in the blast furnace raceway	647
Combustion chamber scaling for energy recovery from furnace process gas: waste to value	657
PACKED BED.....	665
Comparison of particle-resolved direct numerical simulation and 1D modelling of catalytic reactions in a packed bed	667
Numerical investigation of particle types influence on packed bed adsorber behaviour	675
CFD based study of dense medium drum separation processes	683
A multi-domain 1D particle-reactor model for packed bed reactor applications.....	689
SPECIES TRANSPORT & INTERFACES	699
Modelling and numerical simulation of surface active species transport - reaction in welding processes	701
Multiscale approach to fully resolved boundary layers using adaptive grids.....	709
Implementation, demonstration and validation of a user-defined wall function for direct precipitation fouling in Ansys Fluent.....	717

FREE SURFACE FLOW & WAVES	727
Unresolved CFD-DEM in environmental engineering: submarine slope stability and other applications.....	729
Influence of the upstream cylinder and wave breaking point on the breaking wave forces on the downstream cylinder	735
Recent developments for the computation of the necessary submergence of pump intakes with free surfaces	743
Parallel multiphase flow software for solving the Navier-Stokes equations	752
 PARTICLE METHODS	 759
A numerical approach to model aggregate restructuring in shear flow using DEM in Lattice-Boltzmann simulations	761
Adaptive coarse-graining for large-scale DEM simulations.....	773
Novel efficient hybrid-DEM collision integration scheme.....	779
Implementing the kinetic theory of granular flows into the Lagrangian dense discrete phase model.....	785
Importance of the different fluid forces on particle dispersion in fluid phase resonance mixers	791
Large scale modelling of bubble formation and growth in a supersaturated liquid.....	798
 FUNDAMENTAL FLUID DYNAMICS	 807
Flow past a yawed cylinder of finite length using a fictitious domain method	809
A numerical evaluation of the effect of the electro-magnetic force on bubble flow in aluminium smelting process.....	819
A DNS study of droplet spreading and penetration on a porous medium.....	825
From linear to nonlinear: Transient growth in confined magnetohydrodynamic flows.....	831

USING CFD ANALYSIS TO OPTIMISE TOP SUBMERGED LANCE FURNACE GEOMETRIES

Stephen GWYNN-JONES^{1*}, Phil CONRADIE², Stanko NIKOLIC¹, Bennie HENNING², Martin BAKKER¹,
Hugo JOUBERT¹, Brett FRANCIS¹

¹ Tenova PYROMET, Brisbane, QLD, AUSTRALIA

² Tenova PYROMET, Midrand, GAUTENG, SOUTH AFRICA

*Corresponding author's e-mail: Stephen.Gwynn-Jones@tenova.com

ABSTRACT

The gas offtake design is an important aspect of the Top Submerged Lance (TSL) furnace technology. CFD modelling has been used to investigate the gas offtake geometry to better understand and address common industrial issues. The objective of the study was to understand how the shape of the offtake affected emissions from the roof ports, and influenced both the location of the post combustion reactions and the flow profile of the gas within the vessel and waste heat boiler (WHB). The conditions and gas species included in the modelling are based on typical large industrial copper smelters. Commercial software (ANSYS-FLUENT) has been used to investigate design variants by incorporating the effects of momentum, multi-component mixing, radiative and convective heat transfer, combustion reactions, and buoyancy. The learnings from the CFD modelling were integrated into the design of the new Novasmelt™ TSL technology.

Keywords: CFD, TSL, copper smelting, offtake.

NOMENCLATURE

Greek Symbols

ρ Mass density, [kg/m³].

θ Roof angle, [°].

Latin Symbols

P Pressure, [Pa].

T Temperature, [°C].

t Time, [s].

v Velocity, [m/s].

\dot{m} Mass flow, [kg/s].

Sub/superscripts

b Bath inlet.

whb WHB outlet.

fp Feed port opening.

lp Lance port post combustion inlet.

dc WHB downcomer post combustion inlet.

INTRODUCTION

The Top Submerged Lance (TSL) furnace technology was originally developed by the Commonwealth Scientific Industrial Research Organisation (CSIRO) in Australia in the 1970s under the name Sirosmelt (J.M.

Floyd & Conochie, 1984). Originally starting in the field of tin smelting, the technology has since been adopted for copper, lead, nickel and zinc production (J. M. Floyd, 2005), becoming a popular choice for many base metal smelters. The TSL technology involves a cylindrical furnace vessel with material continuously fed via a roof opening into a molten bath. The bath is vigorously stirred by submerged gas injection from the centrally inserted lance. In sulfide smelting TSL furnaces, the bath reactions and bubbling creates a continuous stream of high concentration sulfur dioxide (SO₂) containing off-gas. The off-gas is typically cooled in a waste heat boiler (WHB), often consisting of two vertical radiation shafts and followed by either a spray quencher or a horizontal heat recovery convection section (Köster, 2010). The cooled off-gas is then delivered to an electrostatic precipitator for de-dusting before being sent to an acid plant for sulfur recovery.

The TSL furnace has been the focus of CFD studies in the past, although primarily in the bath region rather than the gas offtake. Morsi et al. (2001) used a CFX model, validated by an experimental setup, of gas injection into a liquid bath to study the impact of gas injection angular momentum (swirl) on the liquid recirculation patterns. Pan and Langberg (2010) used a CFX model and experimental test-work to study the free surface behaviour of large collapsing gas bubbles in a liquid bath (such as those created at the tip of the lance in TSL furnace). Huda et al. (2009) used CFD to study the bath mixing differences when the lance submergence, flow rate and swirl angle were varied. Huda then constructed a model to simulate the submerged zinc fuming reactions that occur in a pilot plant TSL (Huda, Naser, Brooks, Reuter, & Matuszewicz 2012).

Off-gas dynamics has been the subject of study in other copper smelting furnaces. (Pelton, 1995) created a CFD model of the radiation and convection sections of a flash furnace to study the effect of changing the geometry. (Li, Brink, & Hupa, 2009) simulated the particle deposition in a flash furnace WHB radiation section to study locations of accretion formation and resulting impact on heat transfer. However, there appears to be no public domain information specifically addressing the effect of the TSL off-take geometry on the furnace off-

gas flow patterns. This study aims to fill this gap in TSL furnace understanding and discusses how the offtake geometry design can address common industrial issues. The outcomes of this study have been incorporated into the next generation of TSL furnace, the Novasmelt™, with solutions being supplied both to existing operations and for new facilities.

BACKGROUND

TSL Furnace Offtakes

The volume above the bath of the TSL furnace is commonly referred to as the gas offtake. The offtake is shaped to connect the cylindrical barrel section to the roof openings and the gas treatment system. The offtake design must allow for post-combustion reaction management, splash containment, lance and feed entry, and emissions control. Operating TSLs have reported a variety of issues with their offtakes, including: accretion formation, corrosion and steam leakages, feed chute blockages, and roof panel or refractory failures (Bhappu, Larson, & Tunis, 1994; Binengar, 1995; Herrera & Mariscal, 2013; Viviers & Hines, 2005).

There are two main furnace offtake shapes for the TSL vessel in use by industry, a flat roof design and a sloped roof design as shown schematically in Figure 1. Originally the majority of TSL furnaces had sloped roofs, and the flat roof furnace design was introduced to offer cost saving advantages and improve the access for operators when compared to the sloped roof, supposedly without detracting from the off-gas flow dynamics (Arthur & Hunt, 2005). There is no indication in the literature that the latter claim was substantiated, and it is the intent of the present study to address this gap.

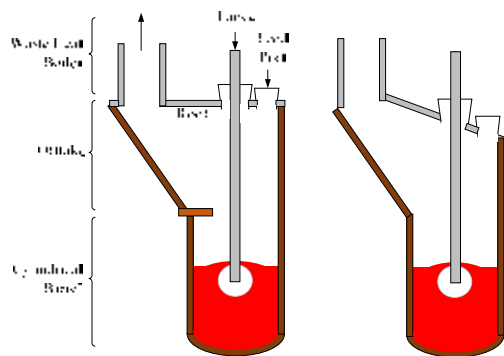


Figure 1: Typical TSL furnace shapes; flat roof design (left), sloped roof design (right)

The materials of construction of TSL furnace offtakes vary in existing designs, with the walls of the offtake typically being refractory lined, although more recently boiler tubes have also been employed (Peippo & Lankinen, 2010). The furnace roof is typically constructed of either copper panels or boiler tubes (Arthur & Hunt, 2005). Refractory bricked furnace offtakes must maintain a minimum shell curvature to ensure brick stability, whereas boiler tubes do not have this restriction and may be shaped to better accommodate fluid flow and remove dead zones. Recently, it has been proposed that additional cost savings could be realised if the entire furnace offtake,

including the walls are manufactured from flat panel boiler tubes, creating a polygonal shape (Peippo & Lankinen, 2010). The effect of the polygonal offtake on the gas flows was not discussed, and it is a further intent of the present work to make use of simplified cases to understand how such a design would impact fluid flow behaviour.

Some flat roof TSL furnace offtakes include a splash mitigation device (Voltura, 2004). The device reduces the amount of splash from the bath that enters the gas offtake and would otherwise form accretion. By providing a physical barrier the splash instead contacts the block, and forms an accretion inside the offtake or returns to the bath. The device is typically a large water cooled copper element. There is no indication that the impact of this geometry on the gas flows within the furnace has been investigated in the literature.

Early TSL furnaces used an angled (rather than vertical) first shaft for the WHB, which resulted in significant issues with accretions. Some of these installations opted to redesign their offtake hood to be vertical to help alleviate these issues (Binengar, 1995; Viviers & Hines, 2005).

Heat Transfer in TSL Furnace Offtakes and WHBs

The WHB is required to cool the off-gas to enable subsequent volatile element precipitation, de-dusting and sulfur recovery from the gas stream. The boiler produces a low pressure steam which requires additional heating for recovery of the heat to power via a turbo-alternator. Alternatively the steam is simply re-condensed. The route chosen by the operation depends on local economics. The heat transfer in this application is complex as high temperature gas (1200 °C), with up to 60 wt. % SO₂ content and laden with reacting dusts, is cooled by a combination of radiative and convective heat exchange with the boiler tube walls. Inside the TSL furnace offtake the heat transfer and combustion reactions are further complicated by three dimensional flow patterns and recirculation. Air/oxygen, at lower temperature than the furnace gases (between 50 – 400 °C depending on whether preheating is used), is usually added to the furnace to provide sufficient oxygen for post combustion reactions. The SO₂ content in the off-gas is the primary species involved in the grey gas radiative heat transfer in the WHB radiation section (Pelton, 1995). Over cooling the gas is problematic, because temperatures below 220 °C can result in weak acid condensation inside the off-take or boiler, leading to corrosion and a loss of sidewall integrity. The boiler water/steam temperature is thus selected, through the boiler pressure setting, to operate above 240 °C to prevent such low temperatures from occurring.

Ingress Air and Draught

Air/oxygen is not only injected into the furnace offtake and boiler, but is also added in a less controlled manner via ingress of additional air through the multiple openings in the furnace as it operates under slight negative pressure. The main source of ingress is air drawn into the open feed port. The negative gauge pressure measured at the port is often called the furnace

draught. Furnace draught is controlled by the downstream off-gas system using an Induced Draught (ID) fan. Engineers typically specify that a TSL furnace should have an ingress air flow rate to suit the process requirements for the off-gas treatment, which results in an off-gas containing 2-2.5 vol% free oxygen at the WHB outlet (Herrera & Mariscal, 2013).

In practice the internal pressure within the TSL vessel fluctuates significantly during operation. At times, the furnace pressure may become positive which results in emission of the furnace gas into the surrounding atmosphere. This is undesirable as these fugitive emissions are hazardous for both the workplace and general environment. Controlling furnace ingress air and preventing fugitive emissions is challenging. The primary causes of the pressure fluctuations within the TSL vessel are predicted to be bath bubble collapse from the submerged lance and the rapid vaporisation of the moisture in the feed as it falls through the furnace top-space. The frequency of the bubble collapse has previously been calculated to be between 1.2-3.4 Hz (Player, 1996), and the magnitude of the pulse will be dependent on the size of the bubble, which is inversely proportional to the bubble frequency. Deeper lance immersion depth has been suggested to increase the bubble size, and reduce the bubble frequency (De Antunes, 2009). The frequency and magnitude of pressure fluctuation from the vaporisation of the feed moisture will be dependent on the stability of the feed rate into the furnace, the moisture content and the homogeneity of the feed.

In addition to the internal causes of TSL furnace pressure fluctuation, there are also external causes. Sulfide smelting TSL furnaces typically interface with complex off-gas handling systems carrying sulfur dioxide laden gases from multiple furnaces to the site sulfuric acid plant(s). If these other furnaces are in batch operating mode, as is typical of converting furnaces (i.e. Peirce-Smith Converters), they can cause rapid changes in the pressure of the entire off-gas system when they roll in or out of the blowing position, requiring ID fan control adjustments to stabilise the TSL furnace pressure. Consequently, the TSL furnace control philosophy requires continual adjustment of the furnace draught in an effort to minimise both excessive accretion in the TSL furnace from too much cold ingress air, and potential release of hazardous fugitive emissions from the furnace ports arising from process pressure spikes.

In the present work, the relationship between furnace draught, bath off-gas flow and ingress air is studied for several different furnace offtake geometries to understand how changing the offtake design affects the gas flows. The different furnace offtake designs are then compared in terms of ability to help achieve process targets and minimise operational issues. Given the current modelling context (complex models exhibiting step change behaviour, qualitative and quantitative targets, limited validation data and lack of directly relevant literature) the analysis is executed using a simplistic approach: changing the design incrementally

and studying the impact. For the sake of brevity, this paper will focus on the findings of the work related to offtake shape. Optimisation for the post combustion air addition (size, quantity, locations, and flow enhancements) and boiler transition piece shapes have been excluded.

MODEL DESCRIPTION

Scope

The CFD model in the present work is intended to focus only on the furnace gas flows. Thus, the model does not consider splash, accretion formation on the walls, or the falling feed. The modelled domain includes the furnace gas space, port openings, WHB uptake, and downcomer. The outlet of the WHB radiation downcomer was set to be of equal height to the feed port.

The geometry used for this study is based on scaling publically available dimensions, drawings and site photos (Chitundu, 2009; Herrera & Mariscal, 2013), and can be considered a reasonable approximation of a typical large TSL copper smelter.

As the intended use of the modelling results was to understand the relative impact of changes, it was decided to limit the complexity to only include the physics that were likely to affect the offtake design.

Main Assumptions

The main assumptions made during the modelling of the gas offtake are:

1. Particulate media are not included in the model to reduce computational time.
2. Heat associated with solid-gas reactions is excluded.
3. Combustion reactions are simplified to include only carbon monoxide (CO), with the remainder of the combustibles recalculated to an equivalent CO flow/concentration as outlined in the process conditions section below.
4. SO₂ reactions are completed in the bath and SO₂ does not participate in the gas-space reactions.

Model Settings

The CFD model was built using the commercial code ANSYS FLUENT[®] 17.2, utilising the pressure-based Navier-Stokes equations. The simulations were set up using a steady state solver approach, with the pseudo-transient option enabled to aid in convergence. The simulation used the k-epsilon 2 equation realizable turbulence model. As the focus was on the macro flow field and small scale recirculation is not expected, the Realizable k-e model was considered adequate for this analysis. Near-wall turbulence was approximated by the accompanying Standard Wall Function and care was taken to maintain an appropriate y+ using three inflation layers for most of the domain. Radiation was implemented using the Discrete Ordinates Radiation Model. The emissivity was calculated depending on the gas composition using the weighted-sum-of-grey-gases model (WSGGM) approach. Due to the high

temperatures inside the furnace, the rate of reaction for the CO oxidation is expected to be primarily controlled by the turbulent mixing. Thus the turbulence/chemistry interactions were modelled using eddy-dissipation, which assumes an instantaneous burn upon mixing. The simulations were executed using double precision. The second order scheme was used for the scalars and energy equations. The PRESTO! Scheme was used for pressure.

Process Conditions

Typical industrial copper smelter process data from the Mt Isa Copper Smelter (Edwards, 1998) was combined with Tenova Pyromet’s in-house copper smelting process model to calculate the gas flows and temperatures. The inputs to this process model were the elemental compositions (Edwards, 1998), which were speciated to their mineralogical components for proper incorporation into the system enthalpy balance. The mineralogical inputs were then bulk reacted to their respective liquid metal oxide slag and liquid metal sulfide matte phases with the remaining sulfur and carbon species partially combusted to the gaseous phase (Yazawa, Nakazawa, & Takeda, 1983). The reaction extents were determined by the output compositional data for the matte grade, mass percent copper in matte, and slag magnetite concentration, as listed in (Edwards, 1998). Combustion of the feed was completed by added air/oxygen, which carries with it both the oxygen for reaction and nitrogen. From a chemical reaction perspective the nitrogen gas component is inert, but this gas is responsible for the generation of bubbles at the end of the submerged lance and therefore ensures the bath is turbulent and that the reactions are completed to their required extents.

The outputs of the process model were converted into the boundary conditions for the CFD model that are specified in **Figure 2**, **Table 1** and **Table 2**. These conditions were kept constant across all of the models to provide a comparison between the different geometries. The thermal boundary condition values were selected based on typical industry values. It should be noted that the gas flow rates and compositions can vary significantly between operations, thus although the findings will hold, the specific flow patterns and calculated outcomes may not apply to operations with significantly different process inputs.

The CO mass flow has been calculated such that it will provide the same total heat energy as all of the other combustible gases arising from the furnace bath (hydrogen, hydrogen sulfide, sulfur gas, methane, etc.). This simplification does not account for the heat energy released from the additional reactions of dust particles entrained in the gas stream. This assumption is not expected to significantly impact on the results.

The wall boundary conditions included heat transfer effects by specifying an effective thermal resistance to the temperatures listed in **Table 2**, and was calculated using a 1D approach based on typical refractory or boiler tube designs. The copper splash mitigation device was set to have the same thermal resistance as the

refractory bricks, based on the assumption that it would be coated in a thick slag layer during operation.

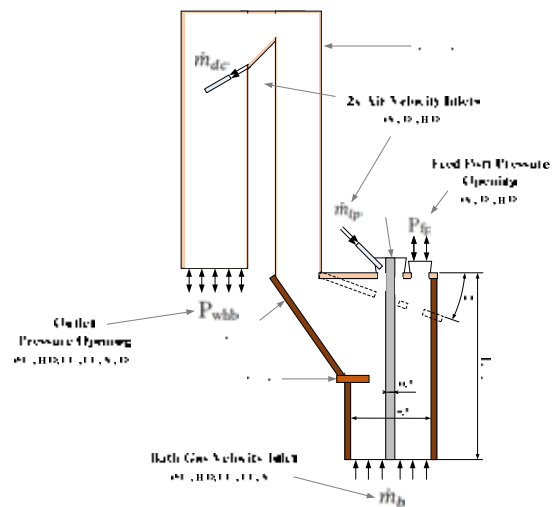


Figure 2: Boundary condition locations and key dimensions on CFD model

Table 1: Fluid boundaries

Boundary Condition	Value	Units	Temperature (°C)
\dot{m}_b	27.4	kg/s	1180
P_{fp}	0	Pa (g)	20
P_{whb}	-100 to -10	Pa (g)	580
\dot{m}_{tp}	1.68	kg/s	50
\dot{m}_{dc}	1.87	kg/s	50

Table 2: Thermal boundaries

Boundary	Heat Transfer Coefficient (W/m ² -K)	Temperature (°C)	Internal Emissivity
Refractory Brick	2.64 ⁽¹⁾	20	0.38 ⁽²⁾
Steel	0 (adiabatic)	NA	1
Boiler Tubes	30 ⁽³⁾	280	0.8 ⁽⁴⁾
Copper	2.64	20	0.38
Bath Inlet	NA	1180	1
Boiler Outlet	NA	580	1

⁽¹⁾ Calculated assuming brick, backing lining and steel layers with natural convection.

⁽²⁾ Magnesite brick emissivity at 1000 °C

⁽³⁾ Typical industrial value for overall heat transfer in TSL WHB

⁽⁴⁾ Combination of frozen slag and oxidised steel surface values

Mesh Strategy

An unstructured tetrahedral mesh was created in ANSYS meshing consisting of approximately 2 million cells. An example of a typical mesh can be viewed in Figure 3. The mesh was refined in the region of the roof ports and post combustion air injection, and inflation layers were used at all walls to capture the boundary layer effects. The tetrahedral mesh was imported into ANSYS FLUENT® and converted to be a polyhedral mesh, reducing the total element count to approximately 0.8 million cells.

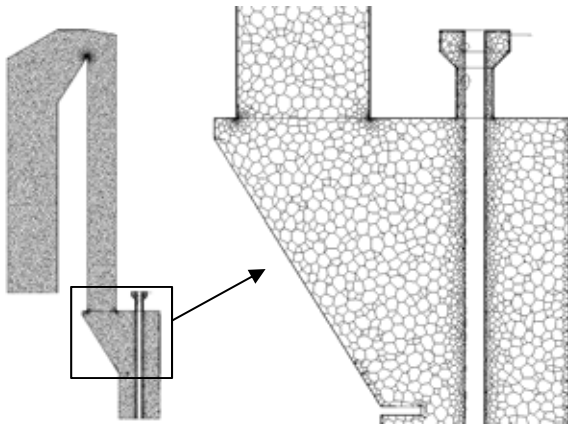


Figure 3: Typical polyhedral mesh on domain centreline. All walls have inflation layers.

Cases

The list of geometry cases is contained in Table 3. The angled roof geometries were created by removing a segment of the offtake volume and lowering the lance and feed ports to suit the angled shape. The flat panel geometries were constructed by matching the offtake width to the WHB. Examples of the geometries are included in Figure 4.

Table 3: CFD Geometry cases

Case	Roof Angle θ ($^{\circ}$)	Offtake Wall Material	Splash Mitigation Device	Offtake Wall	Notes
1.	0	Bricks	Y	Curved Shell	
2.	0	Bricks	N	Curved Shell	
3.	30	Bricks	Y	Curved Shell	
4.	30	Bricks	N	Curved Shell	
5.	0	Boiler Tubes	N	Flat Panels	
6.	15	Boiler Tubes	N	Flat Panels	
7.	30	Boiler Tubes	N	Flat Panels	
8.	45	Boiler Tubes	N	Flat Panels	
9.	45	Boiler Tubes	N	Flat Panels	FP Length x2
10.	0	Bricks	Y	Curved Shell	FP Length x2

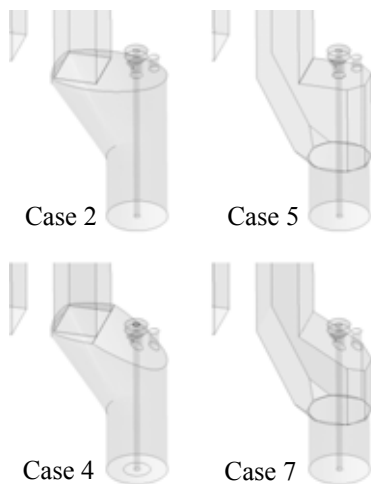


Figure 4: Example geometries for various cases

RESULTS

Convergence

The models typically required 2000 iterations to achieve acceptable convergence from initialisation. Subsequent runs of the same geometry at varying boundary

conditions were run for an additional 1000-1500 iterations depending upon the convergence of the boundary mass flows and temperatures.

Heat Transfer Comparison to Process Assumptions

The process model predicted the WHB radiation section outlet temperature to be approximately 581 °C based on typical operational experience, equating to a total heat loss of 22.1 MW from the boiler tubes and refractory bricks.

The CFD model for Case 1 predicts that the total heat loss through the walls is 15.6 MW by summing the total heat transfer across those surfaces, and is mostly from radiation as shown in Figure 5, which is expected since the model only includes the radiation section of the boiler. When compared to the process model heat loss of 22.1 MW the result indicates that the CFD model may be under-predicting the heat loss in the WHB. While it would have been possible to adjust the heat transfer coefficient for the boiler tubes to be a higher value, the boiler itself is not the focus of the present study. Further, altering the boiler heat transfer was only expected to have a minimal impact on the gas flows in the furnace offtake.

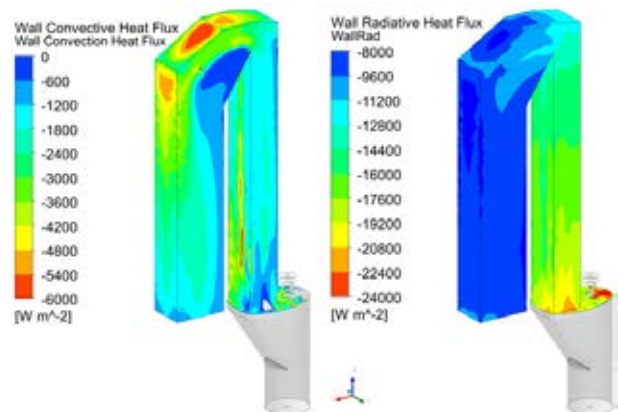


Figure 5: Convective (left) and radiative (right) heat on the boiler tube boundary condition for Case 1 with $P_{whb} = -10$ Pa. Negative heat flux is heat leaving the domain.

Comparison to Site Data

The complexity of the present model requires that it be validated against site data to provide some confidence in its ability to simulate actual furnace conditions. Unfortunately it is only possible to perform limited validation for two reasons: firstly, the geometry and boundary conditions of the CFD model were pieced together from public data sourced from multiple TSL furnaces (Mt Isa, Mopani and SPCC), and secondly, there is limited information in the literature that can be used to validate the CFD predictions. The available plant data for gas temperatures provided by Herrera and Mariscal (2013) are plant measurements from a large scale copper smelter (SPCC) of a similar design throughout to the modelled case.

Case 1 was selected for the model validation as it best matched the offtake design of the Southern Peru Copper Corporation furnace (Cuadros Rojas, 2010). The boiler outlet pressure was set to -10 Pa as this resulted in a

feed port ingress of 2.04 kg/s, where the target value from the process model was 2.05 kg/s.

Figure 6 illustrates the CFD results for temperature cross sections at 12 locations along the WHB. The results show that the CFD model predicts a range of temperatures at each location depending upon the localised flow field.

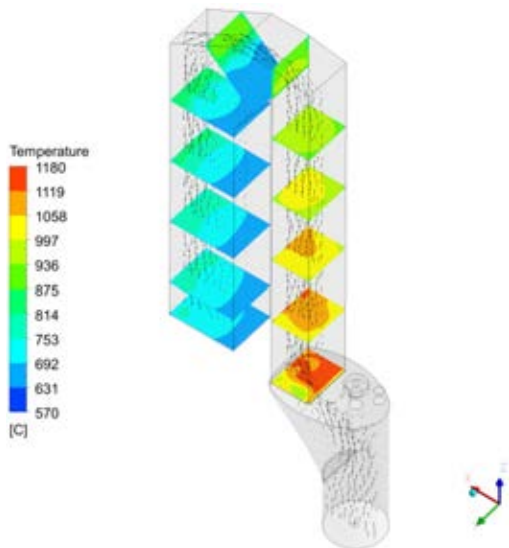


Figure 6: Temperature cross sections along WHB in Case 1 with $P_{whb} = -10$ Pa.

In **Figure 7** the CFD results for temperature at each location are compared against the values from Herrera and Mariscal (2013). As no precise information was provided about the location used to collect the plant temperature measurements, the CFD data is presented as a range for comparison purposes. While the CFD prediction of temperature range overlaps the measured plant data at both measurement locations, the CFD average is higher; this is consistent with the comparison to the process model.

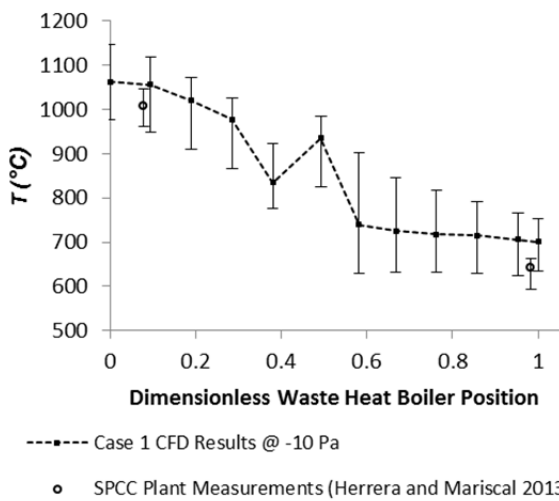


Figure 7: Comparing CFD prediction of off-gas temperature (Case 1 with $P_{whb} = -10$ Pa) to 2 years of copper smelter plant data from Herrera and Mariscal (2013). Error bars on CFD result indicate the range of values of temperatures at each cross section.

There are several reasons that the CFD model might predict slightly different temperatures than the industrial data. The heat transfer coefficient of the boiler tubes used in the model is a typical value, and has not been the subject of rigorous analysis. In the industrial case the curved shape of the boiler tube panels increases the heat transfer area compared to the flat surfaces used in the CFD model. As the boiler is below atmospheric pressure it would be drawing in cold atmospheric air through any openings or gaps between panels, which is not permitted to occur in CFD. Overall the CFD model showed reasonable agreement with site data, indicating it could be used for comparing the relative impact of changes to the geometry.

Impact of a Splash Mitigation Device

The impact of including a splash mitigation device in the design can be assessed by comparing Cases 1 and 2. Note that cases 3 and 4 showed the same change. **Figure 8** shows a velocity contour plot on the furnace centreline. The results indicate that the splash mitigation device creates a large recirculation zone as the rising gas flows around it. The ‘dead zone’ of flow created by the recirculation acts to reduce the effective cross sectional area for the furnace gases, increasing the gas velocity.

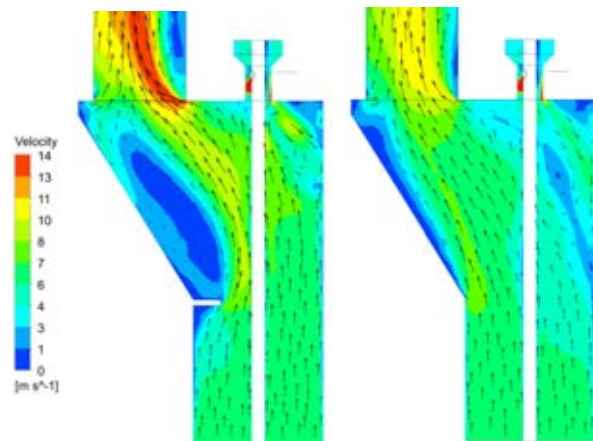


Figure 8: The impact of the splash mitigation device. Velocity contours for case 1 (left) and case 2 (right) at $P_{whb} = -10$ Pa. Splash mitigation device creates large recirculation zone in furnace offtake.

TSL furnace offtakes are typically designed to keep the linear velocity of the gas at the boiler inlet below 10 m/s (Köster, 2010) to ensure homogenous heat transfer and temperature profiles. The presence of the splash mitigation device creates instantaneous velocities up to 14 m/s at the boiler inlet leading to recirculation in the boiler.

Impact of Roof Angle

The air streamlines from the introduction of post combustion air into the furnace lance and feed ports for Cases 1, 2, 3, and 4 are compared in **Figure 9** to understand the impact of adding a slope to the furnace roof and the impact of a splash mitigation device. One of the main differences observable in these results is that the feed port ingress air and the injected lance port air behave differently depending on these geometrical factors. When the roof is flat (Cases 1 and 2), a

recirculation zone is created in the relatively cold stagnant zone below the feed port. The stagnation zone occupies a similar shape to the volume of fluid removed when converting to an angled roof, and is larger when there is no splash mitigation device. When the roof is sloped there is no stagnant zone, and the air is entrained into the furnace gas flow before entering the offtake, and better mixing is observed when there is no splash mitigation device.

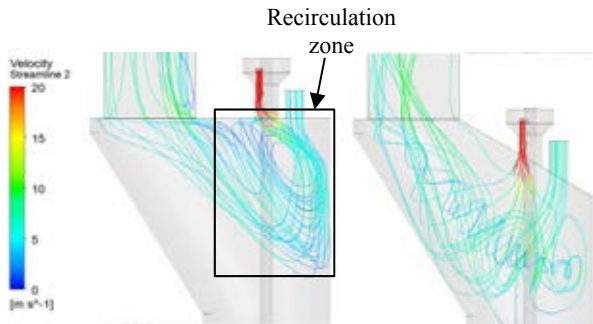


Figure 9: Air streamlines from feed port and lance port post combustion air for case 1 (left), and case 2 (right). Recirculation is evident in the flat roof case.

In order to compare the performance of multiple furnace offtake geometries it is convenient to map the system response for feed port ingress air to changing boiler suction as a series of steady state simulations. The slope of the curve relating ingress air to suction pressure indicates the rapidness with which the furnace will transition from ingress to emission, i.e. “puffing” furnace gas into the atmosphere, for a given pressure pulse.

The simulation results relating the feed port mass flow (\dot{m}_{fp}) to the vessel roof angle (θ) is summarised in Figure 10. The following observations may be made:

- Increasing the slope angle of the roof at a constant -10 Pa at the WHB inlet increases the ingress air flow. This suggests that sloped roof furnaces could run less ID fan suction to meet the same ingress air requirements. The increased angle more effectively channels the gases into the boiler, causing the gas to flow parallel to the roof.
- The presence of a splash mitigation device does not significantly impact the feed port mass flow.

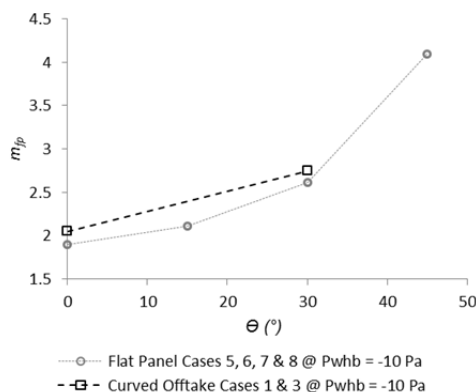


Figure 10: The relationship between feed port ingress air at $P_{whb} = -10$ Pa and vessel roof angle. Increasing the

roof angle increases the ingress air, likely due to increased entrainment.

Flat panel offtake performance

The flat panel boiler tube offtake design is an opportunity to improve the offtake service life, and reduce the complexity and operating costs associated with curved refractory offtakes. Figure 11 and Figure 12 show the air streamlines from the introduction of post combustion air into the lance and feed ports for the curved offtake design (Case 2) and flat panel design (Case 5) for a flat roof TSL. The flat panel geometry reduces the recirculation of the ingress air, likely due to it not having the stagnant zones around the entrance to the boiler as in the curved offtake design. These same benefits were evident in the angled offtake cases that utilised flat panels.

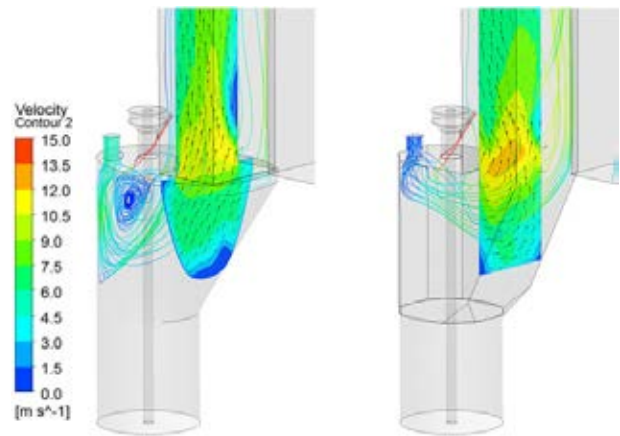


Figure 11: Streamlines and contours showing velocity for Case 2 (left) and 5 (right). The flat panel design has less dead zones around the offtake and fewer recirculation zones.

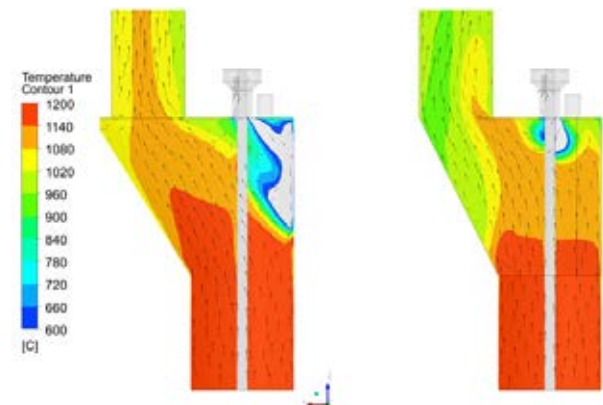


Figure 12: Temperature contours for Case 2 (left) and 5 (right). The inclusion of boiler tube flat panels reduces the gas temperatures in the offtake compared to the bricked design.

Combustion near the splash mitigation device

The results for Case 1, as highlighted previously in Figure 8, show a recirculation region around the splash mitigation device. In conditions representative of higher feed rates there was a deeper penetration of the feed port air combined with the higher volume flow of bath gas generated. The recirculating region is supplied with

oxygen by the feed port air ingress, which results in a combustion zone at the interface with the rising furnace gases. The resulting combustion zone extends the entire length of the splash mitigation device and is in contact with the offtake walls on either side as shown in Figure 13. For refractory furnaces it is suspected that this combustion zone will create local hot spots on the refractory resulting in accelerated wear. This can be mitigated by the application of cooled elements such as plate, SafeCool® or MAXICOOL® coolers (Joubert, Nikolic, Bakker, & McDougall, 2016), which can be retrofitted to existing furnaces. Alternatively boiler tube offtake walls can also perform this function, as investigated in the current work.

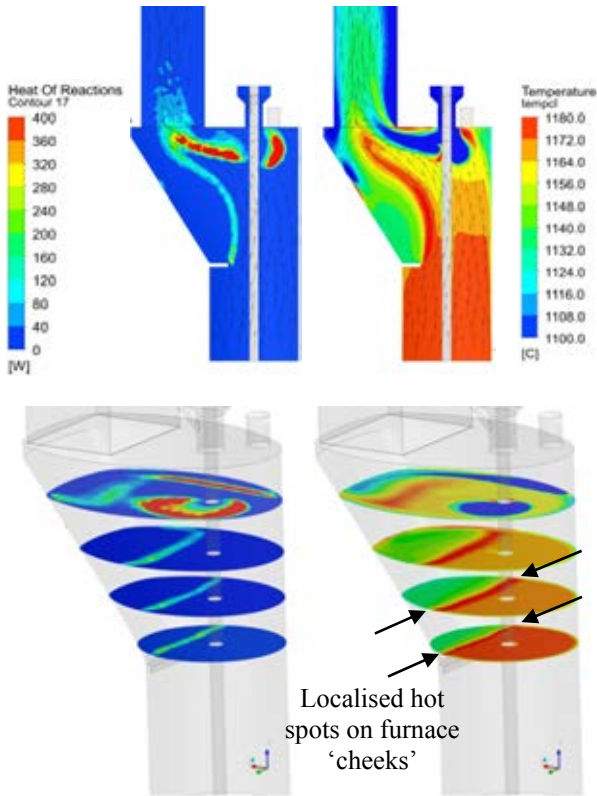


Figure 13: Combustion cross sections (top left and bottom left) and temperature cross sections (top right and bottom right) around the splash mitigation device for Case 1 at $P_{whb} = -40$ Pa for boundary conditions representative of increased feed rates. High localised temperatures around sides of furnace caused by splash mitigation device recirculation region.

Transient simulation of “puffing”

In operating TSL furnaces, the intermittent emission or “puffing” of gases from open ports can occur rapidly and frequently. It is proposed that this puffing is strongly influenced by the bubble collapsing in the bath from the submerged lance gas injection. In order to study this assumption a transient simulation was created. As the bubble frequency has been demonstrated to be related to nitrogen flow, and not the total flow (Player, 1996), it is expected that the bubble expels mainly nitrogen. To simulate these conditions the nitrogen flow rate from the bath was set to fluctuate at +/- 100% from the nominal value in a sinusoidal nature, to provide a generalisation of flow variation due to

bubble collapse. The frequency of the pulsing flow was set at 2 Hz based on the findings of Player (1996).

The boundary conditions used for the transient simulation of bath gas over a one second period are summarised in Figure 14. The simulation was run using FLUENT’s default under-relaxation factors and a time step of 0.025 s. It can be seen that, at its peak, the fluctuating nitrogen component has a similar velocity contribution as all of the other gas species combined.

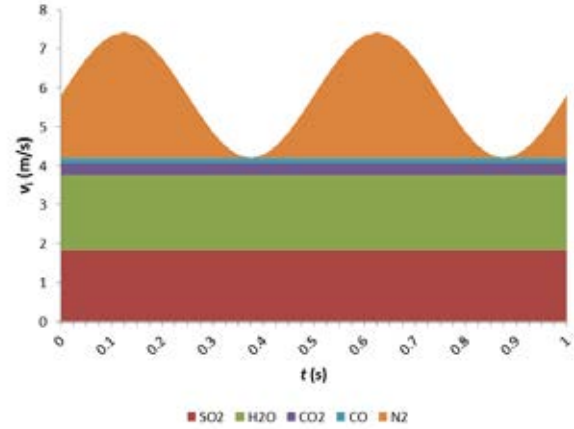


Figure 14: Volume contribution of individual gas species to bath inlet flow velocity for transient simulation case over a 1 second time period. Nitrogen flow is pulsing at 2 Hz.

The results for the total mass flow and mass flow of SO_2 over the feed port boundary with time for case 1 and Case 8 are summarised in Figure 15. SO_2 is selected for this comparison because it is hazardous and is one of the primary constituents of the bath gas. SO_2 is emitted only when the feed port mass flow is net outwards from the domain (negative values). The feed port mass flow can be seen to have a peak when the bath gas velocity has a trough, indicating an inverse relationship. The results also indicate that there is very little difference in performance between the flat roof geometry with splash mitigation device (Case 1) and the 45° angled roof (Case 8), despite the significant geometrical changes to the offtake.

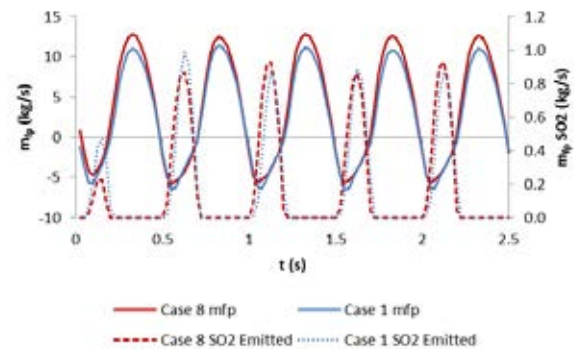


Figure 15: Feed port mass flow for Cases 1 and 8 at $P_{whb} = -10$ Pa in response to pulsing nitrogen flow. Both cases exhibit similar feed port mass flow and SO_2 emissions.

Longer feed port

Additional cases were created to examine the impact of changing the feed port geometry on SO₂ emissions using the transient models. The results of these analyses are summarised in **Figure 16** for Case 9 and 10, which are simply Case 8 and 1 with doubled feed port heights. The results indicate that doubling the feed port height reduces the SO₂ emissions by an order of magnitude. This is because there is insufficient time for the SO₂ to travel along the length of the feed port before the flow is reversed, as per **Figure 17**. This suggests a longer feed port will emit less SO₂ for a given set of pressure pulsing conditions by acting as an increased length buffer zone. In existing TSL furnaces with angled roofs, the layout of the floor levels has resulted in feed port lengths that are approximately twice as long as those found on flat roofed furnaces, perhaps unintentionally conveying these benefits to those operations. Ostensibly the effectiveness of using a longer feed port to reduce puffing will depend on the magnitude of the pulses in the bath gas flow, which will be specific to each operation.

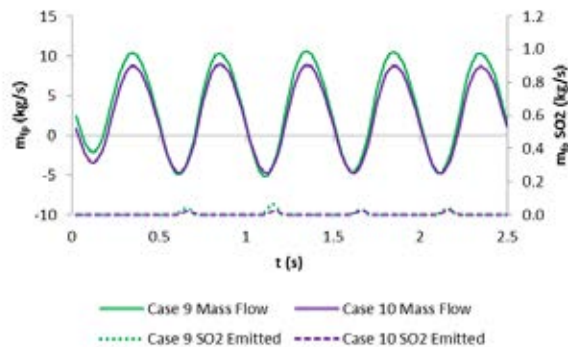


Figure 16: Feed port mass flow for Cases 9 and 10 at $P_{\text{whb}} = -10$ Pa in response to pulsing nitrogen flow. Both cases have 2x feed port length and display a substantial reduction in SO₂ emissions.

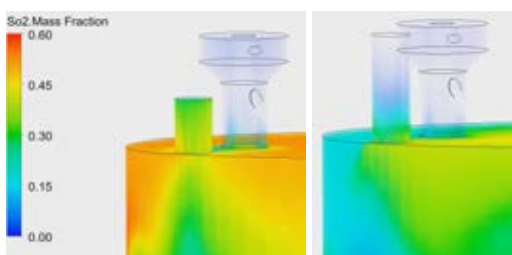


Figure 17: SO₂ mass fraction volume rendering for Case 1 (left) and 10 (right) at $t = 1.625$ s displaying maximum outward mass flow. The longer feed chute exhibits lower SO₂ emissions by increasing the buffer zone.

Dust sulfation and oxidation locations

The off-gas in a TSL furnace is typically laden with dust, which originates from entrainment of small particles or condensation of vapours (Swinbourne, Simak, & Yazawa, 2002). Managing the dust reactions is an important part of designing the off-gas system and post combustion addition. It is important to balance the flows between the furnace and WHB downcomer to prevent accretion formation in the WHB and furnace offtake (Herrera & Mariscal, 2013). While dust

oxidation/sulfation reactions are occurring, the dust is sticky and soft (Ranki-Kilpinen, 2004), which increases the likelihood of accretion formation. In order to predict the regions of accretion formation, temperature contours were added to the Case 8 steady state CFD results to examine the regions where various sulfation reactions are likely to occur (Figure 18). Note that as the CFD model does not incorporate these additional species these contours are only based on the specified temperatures ranges. The results indicate that the simulated WHB would have minimal sulfation reactions occurring in the top of the boiler, reducing the likelihood of accretion formation in this area.

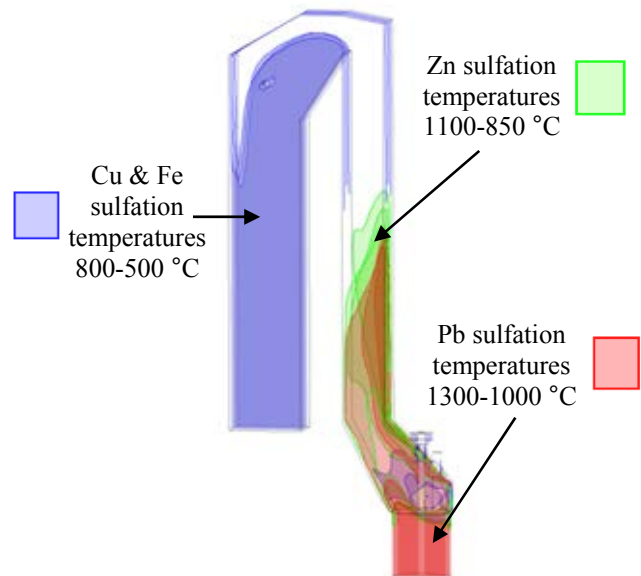


Figure 18: Approximate dust sulfation reaction locations based on temperatures in case 8 at $P_{\text{whb}} = -10$ Pa.

CONCLUSIONS

The TSL furnace gas offtake is an important part of the furnace design that performs a range of essential functions. There is scant evidence in the public domain that the offtake design has been subject to previous rigorous analysis, despite it being the source of numerous issues in operating plants, and the two different designs used throughout industry. The present work has focused on the development of a CFD model that captures key aspects of fluid flow and heat transfer in different TSL furnace offtake geometries. This CFD model was then used to assess the impact of a range of design changes. This CFD model may also be used to investigate off-gas dynamics in existing TSL operations, as long as the site specific boundary conditions and geometry are used.

The learnings from the present work regarding the optimisation of TSL furnace offtakes have been integrated into the new Novasmelt™ TSL design. An optimised TSL furnace offtake geometry would achieve the following:

- Reduction in SO₂ emissions and excessive ingress air from puffing.

- Reduction in damaging post-combustion reactions and ‘hot spots’ near the refractory sidewalls, or use of more robust materials such as boiler tubes.
- Increased homogeneity of flow at inlet to WHB to improve heat transfer and reduce accretion formation.
- Minimise velocities in offtake to reduce carryover of un-smelted feed.
- Sulfation reactions located in vertical sections of boiler to reduce risk of sticky accretion formation in stagnant flow areas.

The following may be concluded from the present work:

1. The inclusion of a splash mitigation device at the bottom of the offtake creates a large recirculation zone, resulting in increased combustion at the furnace sidewalls, higher gas velocities in the offtake, reduced mixing of post combustion air, and less homogenous gas flow in the WHB.
2. Flat roof offtake geometry tends to create a recirculation zone of air underneath the feed port. This can lead to increased carryover, localised accretion formation and thermal shock of the refractory in extreme cases.
3. Angled roof offtake geometry causes ingress air and injected post combustion air to be entrained into the furnace gas bulk flow without recirculation and results in improved mixing.
4. Flat panel offtake geometry using boiler tubes rather than bricks can be used to remove dead zones and reduce gas recirculation, and also results in lower overall temperatures in the offtake.
5. Longer feed ports should result in less furnace “puffing” and significant reductions in SO₂ emissions.

REFERENCES

- ARTHUR, P. S., & HUNT, S. P. (2005). “Isasmelt - 25 Years of Continuous Evolution”, *Paper presented at the John Floyd International Symposium on Sustainable Developments in Metals Processing*, Melbourne, Australia.
- BEZUIDENHOUT, J. J., YANG, Y., & EKSTEEN, J. J. (2008). “Computational fluid dynamic modelling of a waste-heat boiler associated with flash smelting of base metal sulphides” *The Journal of The Southern African Institute of Mining and Metallurgy*, 108(MARCH), 179 - 188.
- BHAPPU, R. R., LARSON, K. H., & TUNIS, R. D. (1994). “Cyprus Miami Mining Corporation Smelter Modernization Project Summary and Status”, *Paper presented at the EPD Congress 1994*.
- BINEGAR, A. H. (1995). “Cyprus Isasmelt start-up and operating experience”. *Paper presented at the Copper 95*, Santiago, Chile.
- CHITUNDU, K. (2009). “Smelter Start-Up of new ISA Furnace and Progress to Date”. *Paper presented at the Presentations from the SAIMM Branch Event*, Chingola, Zambia.
- CUADROS ROJAS, A. (2010). “Reduccion de las Peridadas de Cobre en las Escorias del Proceso IsaSmelt de la Fundicion de Ilo de SPCC”. Universidad Nacional de Ingenieria.
- DE ANTUNES, H. M. A. (2009). “Experimental Study of Lance Bubbling Phenomena”. (Diploma of Engineering), Von Karman Institute, Rhode-Saint-Genève.
- EDWARDS, J. S. (1998). “Isasmelt-A 250 000 TPA Copper Smelting Furnace”. *Paper presented at the AUSIMM '98 - The Mining Cycle*, Mt Isa.
- FLOYD, J. M. (2005). “Converting an idea into a worldwide business commercializing smelting technology”. *Metall. Mater. Trans. B*, 36(5), 557-575. doi:10.1007/s11663-005-0047-7
- FLOYD, J. M., & CONOCHIE, D. S. (1984). “SiroSmelt - The First Ten Years”. *Paper presented at the Symposium on Extractive Metallurgy*, AusIMM, Melbourne, Australia.
- HERRERA, E., & MARISCAL, L. (2013). “Controlling SO₃ Formation in the Off-Gases Process From the IsaSmelt Furnace at Southern Peru Ilo Smelter”. *Paper presented at the Copper 2013*, Santiago, Chile.
- HUDA, N., NASER, J., BROOKS, G., REUTER, M. A., & MATUSEWICZ, R. W. (2009). “CFD Modeling of Swirl and Nonswirl Gas Injections into Liquid Baths Using Top Submerged Lances.” *Metallurgical and Materials Transactions B*, 41B(February 2010), 35-50.
- HUDA, N., NASER, J., BROOKS, G., REUTER, M. A., & MATUSEWICZ, R. W. (2012). “Computational Fluid Dynamic Modeling of Zinc Slag Fuming Process in Top-Submerged Lance Smelting Furnace”. *METALLURGICAL AND MATERIALS TRANSACTIONS B*, 43B, 39-55.
- JOUBERT, H., NIKOLIC, S., BAKKER, M. L., & MCDUGALL, I. (2016). “Tenova Pyromet - Cooled Copper Furnace Elements”. *Paper presented at the Copper 2016*, Kobe, Japan.
- KÖSTER, S. (2010). “Waste Heat Recovery Systems Downstream of Pyrometallurgical Processes for Lead and Zinc”. *Paper presented at the Lead-Zinc 2010*, Vancouver, Canada.
- LI, B., BRINK, A., & HUPA, M. (2009). “CFD Investigations of deposition in a heat recovery boiler: Part II - deposit growth modelling”. *Progress in Computational Fluid Dynamics*, 9(8), 453-459.
- MORSI, Y. S., YANG, W., ACHIM, D., & ACQUADRO, A. (2001). “Numerical and experimental investigation of top submerged gas injection system”. *Transactions on Modelling and Simulation*, 30, 95-104.
- PAN, Y., & LANGBERG, D. (2010). “Two-Dimensional Physical and CFD Modelling of Large Gas Bubble Behaviour in Bath Smelting Furnaces”. *The Journal of Computational Multiphase Flows*, 2(3), 151-164. doi:10.1260/1757-482X.2.3.151
- PEIPPO, R., & LANKINEN, H. (2010). “TSL-Furnace Wall Cooling by Boiler Tubes”. *Presented at Copper 2010*, Vancouver, Canada.
- PLAYER, R. (1996). “Copper Isasmelt - Process Investigation”. *Paper presented at the International symposium, Injection in pyrometallurgy*, Melbourne; Australia.
- RANKI-KILPINEN, T. (2004). “Sulphation of Cuprous and Cupric Oxide Dusts and Heterogeneous Copper Matte Particles in Simulated Flash Smelting Heat Recovery Boiler Conditions”. (Doctor of Science in Technology), Helsinki University of Technology. (TKK-ME-DT-1)
- SWINBOURNE, D. R., SIMAK, E., & YAZAWA, A. (2002). “Accretion and Dust Formation in Copper Smelting - Thermodynamic Considerations”. *Paper presented at the Sulfide Smelting 2002*, Warrendale, PA.
- VIVIERS, P., & HINES, K. (2005). “The New Anglo Platinum Converting Project”. *Paper presented at the First Extractive Metallurgy Operators’ Conference*, Brisbane.
- VOLTURA, S. A. (2004). “Continuous Improvements at the Phelps Dodge Miami Mining Smelter”. *Paper presented at the SME Annual Meeting, Denver, Colorado*.
- YAZAWA, A., NAKAZAWA, S., & TAKEDA, Y. (1983). “Distribution Behaviour of Various Elements in Copper Smelting Systems”. *Paper presented at the Advances in Sulfide Smelting Symposium*.